An Iterative Least-Squares Monte Carlo Approach for the Simulation of Cohort Based Biometric Indices

Anna Rita Bacinello[1†], Pietro Millossovich[1,2†], Fabio Viviano[3*†]

[1*]Department of Economics, Business, Mathematics and Statistics "B. de Finetti", University of Trieste, Piazzale Europa 1, Trieste, 34127, Italy.
[2]Faculty of Actuarial Science and Insurance, Bayes Business School, City, University of London, 106 Bunhill Row, London EC1Y 8TZ, UK.
[3]Department of Economics, Statistics and Finance, University of Calabria, Ponte Bucci Cubo 0 C, Rende, 87036, CS, Italy.

*Corresponding author(s). E-mail(s): fabio.viviano@unical.it;
Contributing authors: bacinel@units.it; pietro.millossovich.1@city.ac.uk;
†These authors contributed equally to this work.

Abstract

This paper tackles the problem of approximating the distribution of future biometric indices under a cohort-based perspective. Unlike period-based evaluations, cohort-based schemes require the computation of conditional expectations for which explicit solutions often do not exist. To overcome this issue, we suggest the application of a well-established methodology, i.e., the Least-Squares Monte Carlo approach. The idea is to approximate conditional expectations by combining simulations and regression techniques, thus avoiding a straightforward but computationally demanding nested simulations method. To show the extreme flexibility and generality of the proposal, we provide extensive numerical results concerning two main longevity indices, life expectancy and lifespan disparity, obtained by adopting both single- and multi-population mortality models. Comparisons between period- and cohort-based results are made as well. Finally, the paper shows that the proposed methodology can be used to approximate other biometric indices at future dates for which cohort-based estimations are often replaced by period ones for computational simplicity.

Keywords: Cohort Biometric Indices, Longevity Risk, LSMC, Stochastic Mortality

1 Introduction

The persistent improvements in mortality rates in most developed countries have become a significant concern for policymakers. The dramatic financial and societal implications of such changes have prompted governments, pension funds and insurance companies to take actions in order to quantify and manage the associated risks.

As Wilmoth [45] noted, the improvement in mortality, and the consequent gain in longevity, is the result of a complex interplay of factors, including technological and medical advancements, better economic and cultural conditions, and political actions aimed at improving lifestyles. In addition, Wilmoth [45] argues that the ever-decreasing trend of mortality levels would lead to an ever-increasing and unbounded life expectancy among individuals. The study of such multifaceted problem is therefore attracting the attention of demographers and actuaries.

To cope with this call, it is nowadays common practice to rely on extrapolative statistical models that use past experience combined with assumptions on the stochastic dynamic evolution of mortality to obtain projections of mortality rates. Deviating from earlier popular approaches based entirely on expert judgements, the Lee-Carter model (see [29]) is a significant milestone that has paved the way for the modern approach to mortality forecasting. Several variants and extensions have then been proposed (e.g., see [7, 37, 38]). For a review and comparison of proposed stochastic mortality models see [8], [22] and [25].

The aforementioned literature focuses on studying mortality from a single population perspective, neglecting any interdependence among populations and/or subpopulations. To fill this gap, [31] proposes a "coherent" model, also known as the Augmented Common Factor (ACF), which is able to capture the short-term divergence and long-term coherence among related subpopulations. In practice, the ACF model exploits a common factor to describe the long-term mortality evolution of the population as a whole, and then incorporates specific parameters to shape the short-term differences among different groups. Since then, various multi-population mortality models have been proposed, such as the well-known gravity model in [14] or the "2-tier ACF" model in [10]. Many other proposals can be found also in [6, 11, 24, 28, 30] and [47].

To synthesize the pattern of mortality several metrics can be used, among which the primary example is the life expectancy. However, this indicator may provide only a partial information on the shape of a mortality curve, especially when comparing two or more populations. For instance, two countries with the same level of life expectancy may be characterized by a different age-at-death distribution. To address this limitation, several indices have been proposed, which aim at measuring the variation in lifespan, such as the Gini coefficient, the life table entropy (see [27]), and the lifespan disparity indicator considered in [19] and [41]. We refer the reader to [40] for a review and comparative study of these and alternative indices.

Whatever the biometric indicator chosen, its future evaluation using stochastic forecasting models typically relies, for computational simplicity, on a period-based approach. This requires simulating a set of period specific mortality rates which are then used to calculate the desired metric. However, these rates refer to different cohorts and therefore implicitly ignore the mortality improvements that would apply after the

valuation date. Mathematically, a full cohort-based approach poses a computational challenge as it involves a conditional expectation. Except for some special cases where mortality is modelled continuously using diffusions with constant coefficients, see for instance [33] and [26], closed-form expressions for these conditional expectations are not available. Using a Monte Carlo approach may be feasible but would involve a nested simulation scheme which may be extremely expensive from a computational perspective or even impracticable if the index must be consistently calculated for different cohorts (e.g., the case of the lifespan disparity index). Dowd et al [12, 13] have first recognized the issue implicit in a cohort-based approach and have proposed a Taylor-series approximation of the conditional expectations to estimate future life expectancy levels. Similarly, Cairns [5] discusses and proposes probit-Taylor approximations to longevity-contingent values to develop dynamic hedging strategies for pension plan liabilities.

In this paper, we claim that a well-established methodology, i.e. the Least-Squares Monte Carlo (LSMC) approach, can be efficiently used to calculate a range of cohort-based biometric indicators. The idea behind the method is to approximate conditional expectations by linear combinations of some basis functions depending on the relevant factors affecting the mortality evolution. The LSMC was first introduced by [9], [39] and [32] in the financial field, and nowadays extensively adopted in the actuarial discipline and practice due to its extreme flexibility and simplicity. For instance, it has been proposed for pricing longevity derivatives (see [4]), and to estimate risk metrics in accordance with the Solvency II regulation as discussed in [21] and [16].

Although the LSMC method has been widely used for approximating conditional expectations involved in various problems, its application to biometric indices has not yet been investigated. The contribution of this paper is twofold. On one hand, we show how the LSMC allows us to simulate future cohort-based biometric indicators under essentially any single or multi-population mortality forecasting model. Using the ACF model for both genders, we highlight, through several examples, the relevance of such an approach and how biased results would be if single population models for each gender are used or if a period-based approach is followed. We focus mainly on two biometric indices: life expectancy that, as discussed in [2], requires a straightforward implementation of the LSMC method since it can be expressed as a simple function of future mortality rates associated to a given cohort, and the widely used lifespan disparity, thus enriching the relevant literature (see, for instance, [15, 34, 42, 46]). On the other hand, we show that some metrics, in particular the lifespan disparity, for which we also extend its definition to the cohort case, can be calculated using either a straightforward application of the LSMC method or through an iterative LSMC based procedure. The latter idea has already been validated and suggested in different contexts, including the valuation of longevity swaps (see [3]) and the time- and market-consistent pricing of participating pension contracts (see [17]). We show that the lifespan disparity can be calculated with a two-stage process in which repeated LSMC estimates of the life expectancy along a given cohort are then combined to seamlessly obtain the wanted metric. We further extend this principle and prove its applicability to any cohort-based biometric index evaluated at the time of death of an individual.

The remainder of the paper is structured as follows: Section 2 introduces the main longevity measures for which we provide some results. Section 3 defines the computational framework and explains briefly the proposed methodology. Section 4 illustrates some numerical results. Finally, in Section 5 we draw some conclusions.

2 Longevity measures

In this Section we introduce two longevity measures, life expectancy and lifespan disparity, both evaluated at a future date under a cohort perspective. The definition depends on the realization of mortality rates after the evaluation date and, as a consequence, requires averaging across these realizations for each possible scenario prevailing at the future date. The benefit resulting from such a more realistic assessment involves however a more elaborate calculation, as opposed to a straightforward period-based metric. Inspired by lifespan disparity, we also consider a general biometric index and explain how it can be evaluated.

Let $\mu_{x;t}$ be the instantaneous death rate at time t for individuals then aged x. As in [8], we assume that the force of mortality is constant over each year of age and calendar, that is, for integers x and t, the following holds:

$$\mu_{x;t} = \mu_{x+s;t+r} \quad \text{for all } 0 \leq s < 1,\ 0 \leq r < 1. \tag{1}$$

Moreover, let $m_{x;t}$ be the central death rate at age x in year t, and $p_{x,t}$ the corresponding one-year survival probability. Therefore, under the assumption (1), the following holds:

$$m_{x;t} = \mu_{x;t}, \qquad p_{x,t} = e^{-\int_0^1 \mu_{x+s;t+s}\mathrm{d}s} = e^{-m_{x;t}}.$$

As future central death rates are not known at time 0 (today), any other index depending on them is an uncertain quantity.

A period-based index for an individual aged x at time $T > 0$ will indeed depend on the sequence of rates

$$m_{x;T},\ m_{x+1;T}, \ldots, m_{x+k;T}, \ldots. \tag{2}$$

Any simulation of these future death rates will provide a realization of the period-based metric. Therefore, simulating from a stochastic mortality model up to and including the date T will generate the statistical distribution of the longevity metric. However, this approach uses a snapshot of the current level of mortality rates across different generations and implicitly assumes a stationary regime.

On the other hand, a definition of a longevity index based on a cohort approach will start by considering the sequence of rates

$$m_{x;T},\ m_{x+1;T+1}, \ldots, m_{x+k;T+k}, \ldots. \tag{3}$$

As the metric must reflect the information available at time $T > 0$, it should be represented as an expectation conditional on that information. We will denote by

$\mathbb{P}_T(\cdot)$ and $\mathbb{E}_T[\cdot]$ the probability and the corresponding expectation, conditional on information available up to and including time T. This information contains the rates $m_{x;t}$ for all x and $t \leq T$.

It is convenient to think of a family $\tau_x(T)$ of stopping times, for nonnegative integers x and T, representing the (curtate) residual lifetime of an individual aged x at time T. It is usually implicitly assumed that, conditional on the information $\mathcal{M}$ resulting from the observation of the mortality rates $m_{x;t}$ for all x and t, the following holds:

$$\mathbb{P}_T\left(\tau_x(T) > h \mid \mathcal{M}\right) = e^{-\sum_{k=0}^{h-1} m_{x+k;T+k}}, \qquad h = 0, 1, 2, \ldots$$

where, as usual, $\sum_a^b \cdots = 0$ when $a > b$. It follows that the h-years survival probability for an individual aged x at time T is

$${}_hp_x(T) = \mathbb{P}_T\left(\tau_x(T) > h\right) = \mathbb{E}_T\left[e^{-\sum_{k=0}^{h-1} m_{x+k;T+k}}\right],$$

see also Eq. (3) in [5].

2.1 Life expectancy

Life expectancy is the average number of years an individual will live starting from a given age and is the most commonly used biometric indicator.

The period life expectancy of an individual aged x at the future time $T > 0$ is defined as follows:

$$e^p_{x,T} = \frac{1}{2} + \sum_{h=1}^{+\infty} {}_hp_{x,T}, \tag{4}$$

where

$${}_hp_{x,T} = e^{-\sum_{k=0}^{h-1} m_{x+k;T}} = p_{x,T} \cdot p_{x+1,T} \cdot \ldots \cdot p_{x+h-1,T}$$

represents the h-years survival probability for an individual aged x at time T, computed by considering the age-specific mortality rates at that date.

We define the cohort life expectancy of an individual aged x at the future time $T > 0$ as

$$e^c_x(T) = \frac{1}{2} + \sum_{h=1}^{+\infty} {}_hp_x(T). \tag{5}$$

Equations (4) and (5) are the discretized versions of the period and cohort life expectancy measures given, for instance, in [20]. Note that

$$e^c_x(T) = \frac{1}{2} + \mathbb{E}_T\left[\sum_{h=1}^{+\infty} \mathrm{e}^{-\sum_{k=0}^{h-1} m_{x+k;T+k}}\right]. \tag{6}$$

2.2 Lifespan disparity

The lifespan disparity, also known as the number of years of life lost, represents the life expectancy lost due to death by an individual and is related to the dispersion of the lifetime distribution.

Starting with the definition given in [36], we define the period lifespan disparity for an individual aged x at the future time $T > 0$ as follows:

$$e_{x,T}^{\dagger,\,p} = \sum_{h=0}^{+\infty} e_{x+h,T}^{p} \cdot \mathrm{e}^{-\sum_{k=0}^{h-1} m_{x+k;T}} \cdot (1 - \mathrm{e}^{-m_{x+h;T}}), \tag{7}$$

where $e_{x+h,T}^{p}$ is defined in Eq. (4).

To obtain the corresponding cohort-based version of this index, consider an individual aged x at time T. The time of death for this individual is $T+\tau_x(T)$, and the age at death is $x + \tau_x(T)$. The resulting expected number of years of life lost, or lifespan disparity, for an individual aged x at the future time $T > 0$, can then be defined as

$$e_x^{\dagger,\,c}(T) = \mathbb{E}_T \left[\tau_{x+\tau_x(T)}(T + \tau_x(T)) \right]. \tag{8}$$

A calculation developed in Appendix A shows that the cohort lifespan disparity can be represented as

$$e_x^{\dagger,\,c}(T) = \mathbb{E}_T \left[\sum_{h=0}^{+\infty} (1 - \mathrm{e}^{-m_{x+h;T+h}}) \sum_{k=1}^{+\infty} \mathrm{e}^{-\sum_{j=0}^{h+k-1} m_{x+j;T+j}} \right] \tag{9}$$

$$= \mathbb{E}_T \left[\sum_{h=0}^{+\infty} e_{x+h}^{c}(T + h) \cdot \mathrm{e}^{-\sum_{k=0}^{h-1} m_{x+k;T+k}} \cdot \left(1 - \mathrm{e}^{-m_{x+h;T+h}}\right) \right], \tag{10}$$

where $e_{x+h}^{c}(T + h)$ is defined in Eq. (5). The second expression mimics Eq. (7) and suggests that an iterative LSMC scheme could be employed for its calculation, where first the cohort life expectancies $e_{x+h}^{c}(T + h)$, $h \geq 0$, are simulated consistently using an LSMC scheme along a given cohort, and then these simulations are used to evaluate Eq. (10), again with an (ordinary) LSMC.

2.3 General biometric index

A general cohort-based mortality index can be defined as

$$Z_x^c(T) = \mathbb{E}_T \left[\Phi(m_{x+j;T+j}, j \geq 0) \right] \tag{11}$$

for some functional Φ of the sequence of cohort-based rates (3) starting from age x at time T. It is clear that both the cohort life expectancy $e_x^c(T)$, see Eq. (6), and the cohort-based lifespan disparity $e_x^{\dagger,\,c}(T)$, see Eq. (9), are special cases of (11), and so is any transform of the residual lifetime $\mathbb{E}_T \left[f(\tau_x(T)) \right]$, for some function $f : \mathbb{R} \to \mathbb{R}$. Similarly to what done with the lifespan disparity, one can consider the value of such

an index at the future time of death of an individual aged x at T, that is

$$\mathcal{Z}^c_x(T) = \mathbb{E}_T[Z^c_{x+\tau_x(T)}(T + \tau_x(T))].$$

This index would then give the value of the index $Z^c_\cdot(\cdot)$ lost due to death of an individual aged x at T. A calculation similar to that in the previous section allows to use the following representation, which lends itself to an iterative LSMC scheme:

$$\mathcal{Z}^c_x(T) = \mathbb{E}_T\left[\sum_{h=0}^{\infty} Z^c_{x+h}(T+h)e^{-\sum_{j=0}^{h-1} m_{x+j;T+j}}(1 - e^{-m_{x+h;T+h}})\right].$$

3 Model framework

As seen in Section 2, forecasting longevity metrics, both period- and cohort-based, requires projections of mortality into the future. Since the comparison between lifetime characteristics of different groups or populations is extremely relevant in many contexts, we use multi-population stochastic mortality models to achieve consistent future mortality projections. We also consider single-population stochastic mortality models, which entail independent projections, in order to illustrate the possible bias resulting from neglecting the dependence between biologically related groups.

3.1 Stochastic mortality models

To capture a variety of forecasting models, we adopt the following framework. Let $X_t, t = 0, 1, \ldots$, be a vector of stochastic processes of relevant risk factors affecting the mortality dynamics of the set of populations. The vector X_t may include unidentified factors, as in many extrapolative mortality models, or other variables, such as GDP, as in [35]. Without loss of generality, (X_t) is assumed to be a (possibly non-homogeneous) Markov process living on some probability space $(\Omega, \mathcal{F}, P)$.

Let $i = 1, \ldots, I$ be the index denoting the specific population considered and $m_{x;t;i}$ the central death rate at age x in calendar year t of an individual in this population. We assume that

$$m_{x;t;i} = f(t, x, X_t, i) \tag{12}$$

for some function f. The vector X_t may include variables that are specific to the i-th group or are common to the set of I populations. The association between different groups may be explicit, due to the presence of common factors, or implicit, through the dependence within the vector X_t.

When each population has a dedicated subvector $X_{t;i}$ of variables, so that

$$m_{x;t;i} = f(t, x, X_{t;i}, i),$$

and the vectors $(X_{t;1}, \ldots, X_{t;I})$ are independent, then we are back to the case of single population modelling where each group is specified separately from the others.

This formulation encompasses most extrapolative stochastic mortality models proposed in the literature. Among the single population models, it includes the Lee-Carter

and its extensions, the CBD family of models (specified through central death rates), the Plat model and, more generally, the GAPC class of mortality projection models (see [23, 44]), provided the time indices are Markov processes (which is usually the case with ARIMA-type processes when the state space is expanded). It also includes most multi-population models such as the Common Factor and Augmented Common Factor, and relative approaches such as the gravity model, see [43] for a review.

In particular, in the numerical examples we will use the (single population) Lee-Carter model and the Augmented Common Factor model. We denote the number of deaths at age x in year t of the i-th population with $D_{x;t;i}$, and assume it is Poisson distributed with parameter $E_{x;t;i}m_{x;t;i}$, where $E_{x;t;i}$ represents the central exposure. The single population Lee-Carter (LC) stochastic mortality model for the i-th group is specified as follows:

$$\log m_{x;t;i} = \alpha_{x,i} + \beta_{x,i}\kappa_{t,i},$$

where $\alpha_{x,i}$ is an age-specific parameter, $\kappa_{t,i}$ is a period index dictating the mortality decrease over time, and $\beta_{x,i}$ modulates the effect of the period index across ages. In order to project mortality over time, the period index $\kappa_{t,i}$ is usually assumed to be a random walk with drift,

$$\kappa_{t,i} = \delta_i + \kappa_{t-1,i} + \epsilon_{t,i},$$

where δ_i is the drift parameter, and $\epsilon_{t,i}$ is a Gaussian error term with mean 0 and variance $\sigma^2_{\epsilon,i}$. The error terms of different populations are independent. The vector of state variables is then $X_t = (\kappa_{t,1}, \ldots, \kappa_{t,I})$.

A multi-population extension of the LC model is the Augmented Common Factor (ACF) model, proposed by [31]. Under this setting, the central death rate is specified as follows:

$$\log m_{x;t;i} = \alpha_{x,i} + B_x K_t + \beta_{x,i}\kappa_{t,i},$$

where $B_x K_t$ is the common factor among the populations, and $\beta_{x,i}\kappa_{t,i}$ is the subpopulation-specific factor. The common time index, K_t, depicts the overall mortality time trend, and B_x modulates its effects across ages. The factor $\beta_{x,i}\kappa_{t,i}$, instead, allows for a short or medium-term difference between the rate of change in the i-th sub-population death rates and that implied by the common factor.

According to Li and Lee [31], the period index K_t can be assumed to follow a random walk with drift independent from the subpopulation-specific time parameters $\kappa_{t,i}$; instead, the latters are usually modelled as autoregressive processes with order 1, which avoids a long-term divergence in mean mortality forecasts. Formally,

$$\begin{aligned} K_t &= d + K_{t-1} + \epsilon_t, \\ \kappa_{t,i} &= \gamma_{0,i} + \gamma_{1,i}\kappa_{t-1,i} + \epsilon_{t,i}, \end{aligned}$$

where d, $\gamma_{0,i}$ and $\gamma_{1,i}$ are constants with $|\gamma_{1,i}| < 1$, and ϵ_t is a white noise process independent of the white noise processes $\epsilon_{t,i}$, for all i. The vector of state variables is in this case $X_t = (K_t, \kappa_{t,1}, \ldots, \kappa_{t,I})$.

3.2 Valuation procedure

As shown in Section 2, cohort-based valuations of both future life expectancy and lifespan disparity require computing conditional expectations. This is not a trivial task, since explicit expressions often do not exist. In particular, this is the case for many mortality models referenced in Sec. 3.1 and in particular for the LC and the ACF. For this reason, a straightforward approach would rely on simulations based methods, and specifically on a nested simulations scheme, see [18], which is, however, computationally challenging. Indeed, it consists in generating several outer scenarios of mortality rates at the future time T, for each of which a further number of simulations branch out, the so-called inner trajectories. The conditional expectation is then evaluated by averaging across the inner paths.

A possible way to avoid the nested simulations has been proposed by Dowd et al [12, 13], where conditional expectations are approximated by a Taylor-series expansion. However, even this approach would be time-demanding since multiple simulation sets are needed in order to estimate the involved partial derivatives. This becomes more apparent when valuations are required for different ages and/or future calendar years.

For this reason, we propose the adoption of a very flexible tool for approximating conditional expectations, i.e. the Least-Squares Monte Carlo (LSMC) method. The main idea of the LSMC approach is to express conditional expectations as linear combinations of some basis functions (e.g. simple or orthogonal polynomials) evaluated on the relevant risk factors, X_t, that affect the evolution of mortality, and use regression across simulations against those factors. The LSMC algorithm, in the context of Equations (5) and (10), is described in Appendix B. Moreover, for further details on the accuracy of the LSMC method we refer the reader to [1], where a similar approach has been exploited to evaluate life annuities.

4 Numerical Results

In this Section, we provide some numerical results based on the previously introduced framework. In particular, we analyse the evolution of life expectancy and lifespan disparity with both cohort and period life tables. The analysis considers the Italian population, both males and females, and exploits single (LC) and multi-population (ACF) mortality models. The models have been calibrated using the **R** package **StMoMo** (see [44]) on the mortality data over the period $1965-2016$ and ages $35-89$ obtained from the Human Mortality Database. Note that, under the LC setting, the model has been independently fitted on the gender-specific data. We assume that year 2016 is today, and that life tables are closed by a log-linear procedure up to the ultimate age $\omega = 120$. Finally, all the computations are based on $n = 20000$ trajectories, and the LSMC algorithm exploits as basis functions simple polynomials of degree p depending on the adopted mortality model, i.e. $p = 3$ for the LC model and $p = 2$

for the ACF, which corresponds to the same number of basis functions, $M = 10$.[1] Finally, the quantities of interest are evaluated for individuals (males and females) aged $x = 65$ at times $T = 2017, \ldots, 2050$. In Appendix B we describe the algorithms which have been used to obtain the results. Clearly, the numerical examples depend on the adopted mortality models and will be interpreted accordingly. Nonetheless, due to the strong flexibility of the LSMC algorithm, alternative, more complex dynamics to describe the evolution of mortality can be used. Table 1 summarizes the figures and tables containing the numerical results.

Table 1 Map of tables and figures based on index (LE=life expectancy, LD=lifespan disparity), approach (c=cohort, p=period), gender (m=males, f=females) and model (LC=Lee-Carter, ACF=Augmented-Common-Factor).

	description	index	approach	gender	model
Table 2	summary of distribution	LE	c	f	LC, ACF
Table 3	summary of distribution	LE	c	m	LC, ACF
Fig. 1	density	LE	c	m, f	LC, ACF
Fig. 2	fan chart by model	LE	c	m, f	LC, ACF
Fig. 3	fan chart by gender	LE	c	m, f	LC, ACF
Fig. 4	mean trend	LE	c	m, f	LC, ACF
Fig. 5	ratio f/m mean trends	LE	c	-	LC, ACF
Fig. 6	fan chart by approach	LE	c, p	m, f	ACF
Table 4	mean value	LE	c, p	m, f	ACF
Fig. 7	mean trend by approach	LE	c, p	m, f	ACF
Table 5	summary of distribution	LD	c	f	LC, ACF
Table 6	summary of distribution	LD	c	m	LC, ACF
Fig. 8	density	LD	c	m, f	LC, ACF
Fig. 9	fan chart by model	LD	c	m, f	LC, ACF
Fig. 10	fan chart by gender	LD	c	m, f	LC, ACF
Fig. 11	fan chart by approach	LD	c, p	m, f	ACF
Table 7	mean value	LD	c, p	m, f	ACF
Fig. 12	mean trend by approach	LE	c, p	m, f	ACF
Fig. 13	fan chart by index	LE, LD	c	m, f	ACF

4.1 Life Expectancy

We start by considering the future cohort life expectancy evaluated according to Equation (5). Tables 2 and 3 report a summary of the resulting distributions for females and males aged $x = 65$ at different future years T, respectively.

Regardless of the model employed, the distributions tend to shift to the right, reflecting the longer life span as time goes by. Also, the distributions become more dispersed while preserving a symmetric light-tailed shape, as confirmed by Figure 1. Further, the LC model generates future expected lifetimes for males lower than those implied by the ACF while the opposite happens for females. This is due to the fact that the independent LC does not account for the joint trend in males and females, unlike the ACF. Figure 1 clearly shows that, as expected, the distribution of males future life expectancy is dominated by the corresponding distribution for females for both the LC and ACF models.

[1] The number of basis functions is $M = \sum_{k=0}^{p} \binom{r+k-1}{k}$, where r denotes the number of factors, i.e. covariates used in the regression. In particular, $r = 2$ (i.e., $\kappa_{T,\mathrm{f}}$ and $\kappa_{T,\mathrm{m}}$) in the LC setting, and $r = 3$ (i.e., K_T, $\kappa_{T,\mathrm{f}}$ and $\kappa_{T,\mathrm{m}}$) in the ACF.

Table 2 Summary of the distribution of cohort life expectancy $e_x^c(T)$ for females aged $x = 65$ at time T under the LC and ACF models.

		mean	sd	skewness	kurtosis	5^{th} perc.	median	95^{th} perc.
$T = 2017$	LC	25.01	0.21	-0.02	3.15	24.67	25.01	25.36
	ACF	24.39	0.17	-0.04	3.02	24.11	24.39	24.67
$T = 2028$	LC	26.50	0.67	-0.12	3.00	25.36	26.52	27.58
	ACF	25.73	0.55	-0.01	3.00	24.83	25.73	26.64
$T = 2039$	LC	27.91	0.89	-0.13	3.02	26.42	27.92	29.34
	ACF	27.00	0.73	-0.07	2.98	25.78	27.01	28.19
$T = 2050$	LC	29.23	1.02	-0.16	3.08	27.52	29.26	30.86
	ACF	28.19	0.84	-0.10	3.00	26.79	28.20	29.54

Table 3 Summary of the distribution of cohort life expectancy $e_x^c(T)$ for males aged $x = 65$ at time T under the LC and ACF models.

		mean	sd	skewness	kurtosis	5^{th} perc.	median	95^{th} perc.
$T = 2017$	LC	20.73	0.15	0.01	2.75	20.48	20.73	20.98
	ACF	20.66	0.19	-0.01	3.03	20.34	20.66	20.98
$T = 2028$	LC	21.98	0.50	-0.08	3.01	21.15	21.99	22.79
	ACF	22.14	0.64	-0.01	2.99	21.08	22.14	23.20
$T = 2039$	LC	23.17	0.66	-0.12	2.96	22.06	23.19	24.23
	ACF	23.59	0.86	-0.05	2.98	22.16	23.59	24.98
$T = 2050$	LC	24.30	0.76	-0.13	2.93	23.03	24.32	25.53
	ACF	24.97	0.99	-0.09	2.99	23.32	24.98	26.57

The previous findings are confirmed by Figures 2 and 3 which display fan charts of the evolution of cohort life expectancy distributions at future dates $T \in \{2017, \ldots, 2050\}$. Fan charts make the analysis clearer and more effective since they show ranges of possible future values along with most likely outcomes (dark shadows). Moreover, as stated in [12], fan charts help in highlighting the uncertainty which usually characterizes the evolution of longevity indices. Specifically, Figure 2 shows the extent of the more pessimistic scenarios resulting from the LC model for males and the corresponding more optimistic ones for females. Further, the figure allows to capture the higher uncertainty in female future life expectancy over that implied by the ACF model, and the opposite situation for males. It can be noted from the right-hand plot that the 90% prediction intervals provided by both models almost overlap throughout the entire forecast period, while the upper bounds are markedly different. Figure 3 provides an understanding of how projections differ if dependence in populations is allowed for or not. In particular, under the LC model, the relationship between male and female life expectancy reflects the assumed lack of correlation. The ACF, instead, shows a more composite pattern stemming from the common time factor affecting mortality rates of both genders jointly.

In this regard, it is worth noting that, looking at the right-hand side of Figure 3, the lower bound of the 90% prediction interval for females central forecasts is about to overlap the upper bound relative to male forecasts.

Figure 4 reports the observed and projected mean trend of future life expectancy for both genders and models in 1966-2050. Note that, for cohorts aged $x = 65$ up to 1992, life expectancy has been calculated directly from (fitted) mortality rates; for cohorts aged $x = 65$ in 1993-2016, it has been evaluated with standard Monte Carlo;

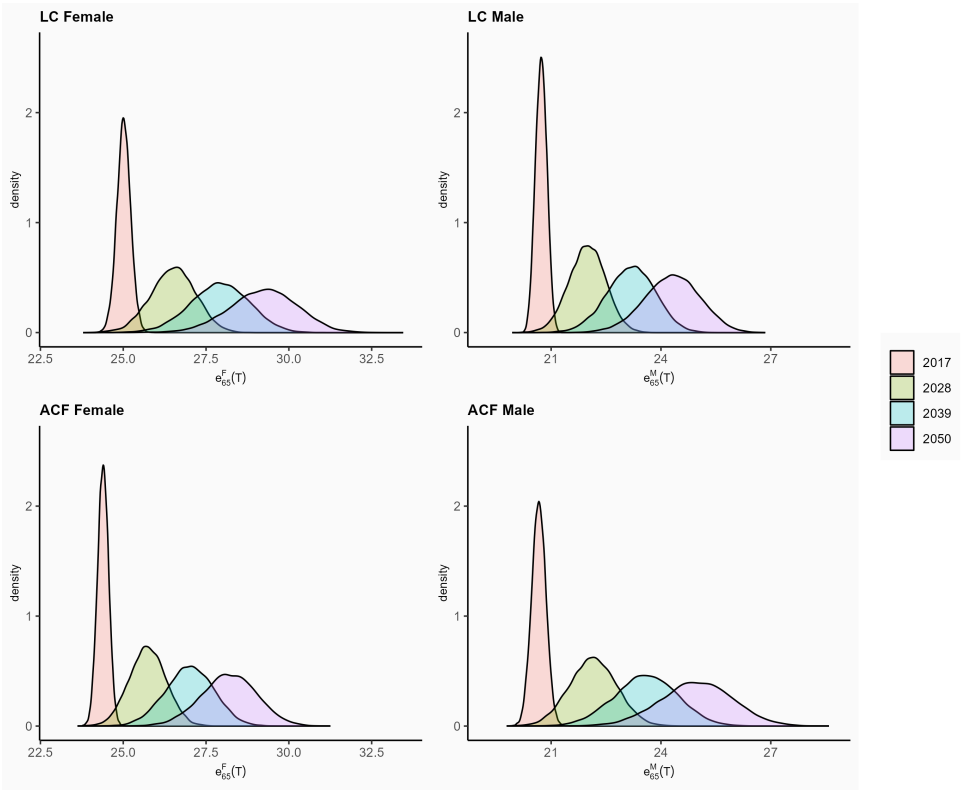

Fig. 1 Probability density function of cohort life expectancy $e^c_x(T)$ for females (left) and males (right) aged $x = 65$ at times $T = 2017, 2028, 2039, 2050$. LC model (top), ACF model (bottom).

finally, for the remaining cohorts, the LSMC algorithm has been used. It is evident the impact of long-term divergence which usually characterizes independent projections (see [31]). Indeed, the gap between male and female LC estimates is wider than the corresponding ACF one. Figure 5 confirms that recent historical trends result in a remarkable reduction of life expectancy between the two genders if the presence of common mortality drivers is allowed for. The independent projections, instead, seem to imply a much more stable relation.

Finally, we focus on the difference between projections obtained by a cohort or a period approach, limiting the discussion to the more comprehensive ACF model. The valuation under the period approach has been made according to Equation (4). Figure 6 displays the corresponding fan charts of future life expectancy. The extent of the systematic underestimation resulting from disregarding the full pattern of mortality improvements is strikingly evident. The magnitude of such phenomenon can be appreciated from Table 4 and Figure 7, further strengthening the motivation for the use of a cohort-based assessment, in particular when decisions in the public social system must be made. On average, the period-based projections of the expected future lifespan are consistently lower than the cohort-based ones by about 2 years for females and 1.5 years for males.

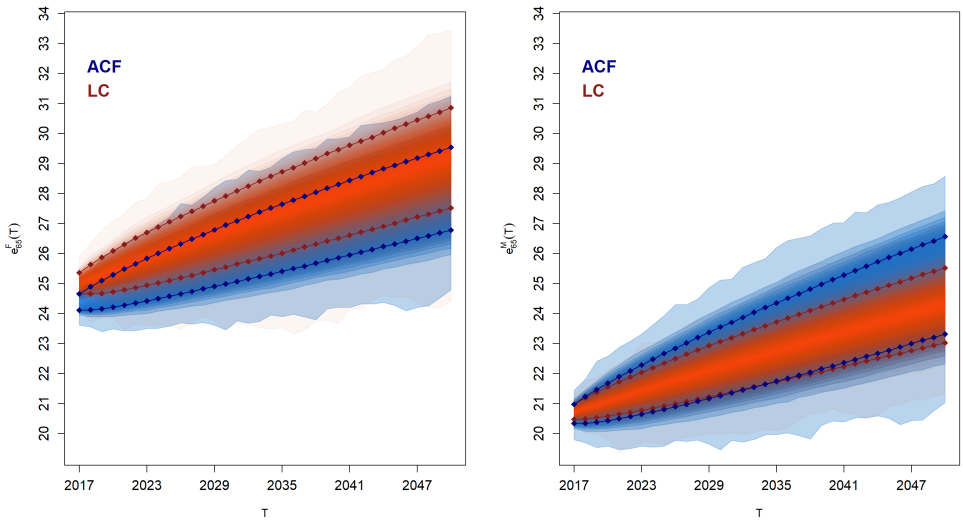

Fig. 2 Fan charts of the distribution of cohort life expectancy $e_x^c(T)$ for females (left) and males (right) aged $x = 65$ at times $2017 \leq T \leq 2050$. LC model (red) and ACF model (blue).

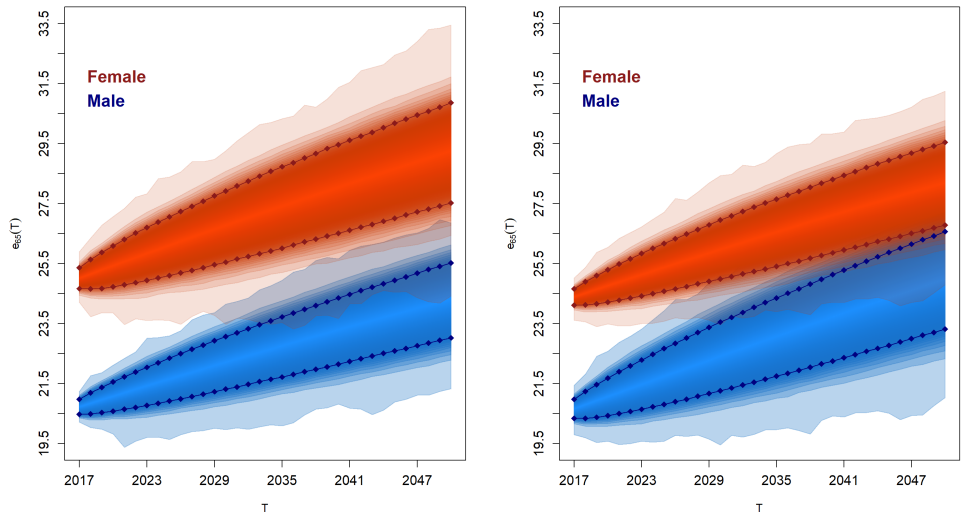

Fig. 3 Fan charts of the distribution of cohort life expectancy $e_x^c(T)$ for females (red) and males (blue) aged $x = 65$ at times $2017 \leq T \leq 2050$. LC model (left) and ACF model (right).

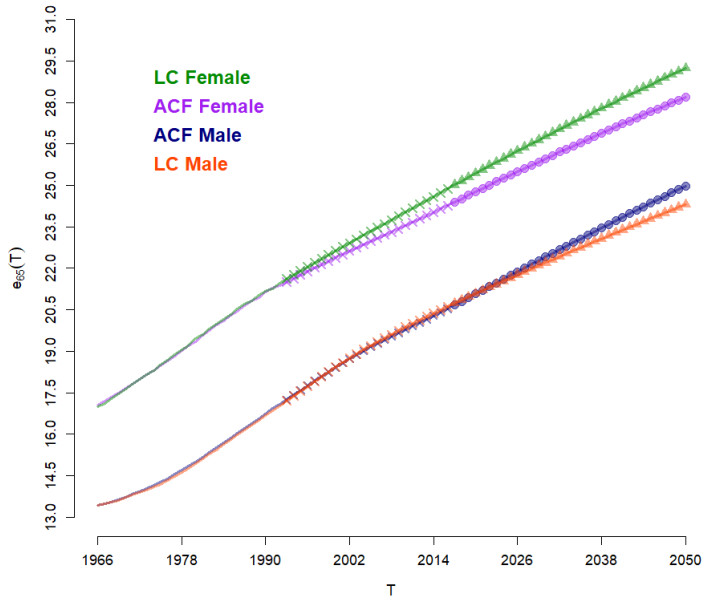

Fig. 4 Expected cohort life expectancy $\mathbb{E}[e_x^c(T)]$ for females and males aged $x = 65$ at times $1966 \leq T \leq 2050$. The solid lines are estimated with the fitted mortality rates. The solid lines marked by crosses represent Monte Carlo estimates. The solid lines marked by triangles (LC model) and circles (ACF model) refer to the LSMC estimates.

Table 4 Expected cohort and period life expectancy, $\mathbb{E}[e_x^c(T)]$ and $\mathbb{E}[e_{x,T}^p]$, for females and males aged $x = 65$ at time T under the ACF model.

		female	male
$T = 2017$	period	22.49	19.06
	cohort	24.39	20.66
$T = 2028$	period	23.86	20.43
	cohort	25.74	22.14
$T = 2039$	period	25.15	21.81
	cohort	27.00	23.59
$T = 2050$	period	26.37	23.16
	cohort	28.19	24.97

4.2 Lifespan disparity

We consider now the projection of future cohort lifespan disparity, calculated as in Equation (10). As discussed in the literature, most industrialized countries have been experiencing ever-increasing trends in life expectancy and, simultaneously, lowering uncertainty of the age-at-death distribution (e.g., see [42, 46]). This composite effect has led to a change in the pattern of lifespan disparity. This indicator, which had been growing steadily since the post-war years, has in recent years reversed its trend

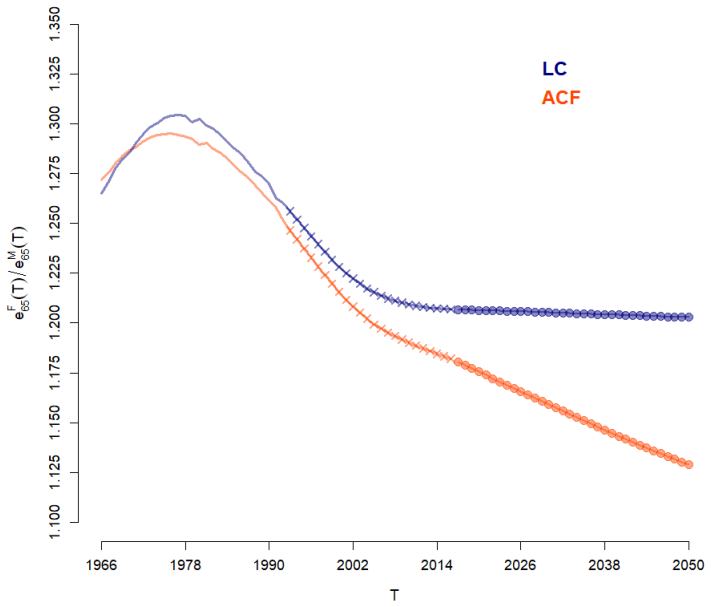

Fig. 5 Ratio between expected cohort life expectancies for females and males aged $x = 65$ at times $1966 \leq T \leq 2050$ under the LC and ACF models. The solid lines are estimated with the fitted mortality rates. The solid lines marked by crosses represent Monte Carlo estimates. The solid lines marked by circles refer to the LSMC estimates.

which is then carried on by extrapolative mortality models, as shown in the following examples. Tables 5 and 6 report a summary of the resulting distributions for females and males aged $x = 65$ at different future years T, respectively. The corresponding probability densities can be found in Figure 8. In each considered configuration, the location of the lifespan disparity distribution decreases while its dispersion increases with the forecast horizon. The ACF model projects a lifespan disparity for males on average higher than the corresponding value for females. Beyond this, the results based on the LC model are very close to those of the ACF, as can be appreciated from Figure 9, where the fan charts are essentially overlapping on the left-hand side while they follow clearly different central trends on the right-hand side. By looking at Figure 10, it is apparent that the ACF model is able to capture a finer relation existing between lifespan disparity of males and females, once again justifying the effort required by a multi-population mortality model.

Figure 11 compares the distributions of future cohort and period lifespan disparity by gender. Note that the valuation under the period approach is based on Equation (7). It can be seen that period-based forecasts result in a completely different pattern, underestimating the level and failing to evidence the decreasing trend of the index. The extent of these differences can be appreciated also from Table 7. Further, the variability of these distributions is lower than that with a cohort perspective.

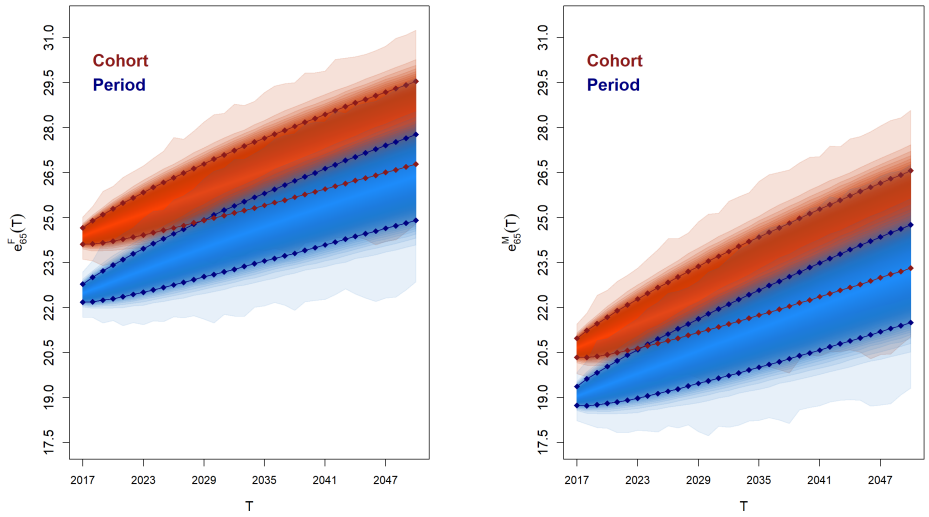

Fig. 6 Fan charts of the distribution of cohort (red) and period (blue) life expectancy, $e^c_x(T)$ and $e^p_{x,T}$, for females (left) and males (right) aged $x = 65$ at times $2017 \leq T \leq 2050$ under the ACF model.

Table 5 Summary of the distribution of cohort lifespan disparity $e^{c,\dagger}_x(T)$ for females aged $x = 65$ at time T under the LC and ACF models.

		mean	sd	skewness	kurtosis	5^{th} perc.	median	95^{th} perc.
$T = 2017$	LC	8.14	0.01	-0.10	2.69	8.12	8.14	8.16
	ACF	8.10	0.01	0.06	3.08	8.08	8.10	8.11
$T = 2028$	LC	8.04	0.05	-0.25	2.96	7.95	8.04	8.12
	ACF	8.02	0.04	-0.18	3.05	7.95	8.02	8.07
$T = 2039$	LC	7.92	0.08	-0.22	2.84	7.77	7.92	8.04
	ACF	7.92	0.06	-0.22	3.06	7.82	7.92	8.02
$T = 2050$	LC	7.78	0.11	-0.15	2.94	7.60	7.78	7.96
	ACF	7.82	0.08	-0.16	3.03	7.68	7.82	7.94

Table 6 Summary of the distribution of cohort lifespan disparity $e^{c,\dagger}_x(T)$ for males aged $x = 65$ at time T under the LC and ACF models.

		mean	sd	skewness	kurtosis	5^{th} perc.	median	95^{th} perc.
$T = 2017$	LC	8.09	0.01	0.11	3.63	8.07	8.09	8.10
	ACF	8.43	0.00	0.81	4.34	8.43	8.43	8.43
$T = 2028$	LC	8.01	0.03	-0.19	2.92	7.95	8.01	8.07
	ACF	8.41	0.02	-1.02	4.34	8.37	8.41	8.44
$T = 2039$	LC	7.92	0.05	-0.12	2.93	7.83	7.92	8.01
	ACF	8.35	0.05	-0.68	3.66	8.27	8.36	8.42
$T = 2050$	LC	7.82	0.07	0.01	2.95	7.71	7.82	7.94
	ACF	8.27	0.07	-0.43	3.25	8.14	8.27	8.38

To highlight how the different approaches impact the projections, Figure 12 shows the corresponding average trend over the entire time horizon 1966-2050. It is confirmed how, even for the initial period where calculations can be done exactly or using a simple

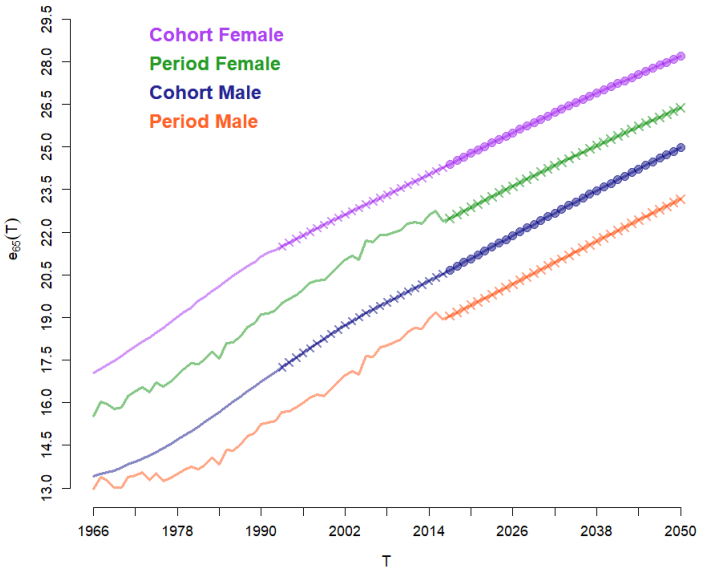

Fig. 7 Expected cohort and period life expectancies, $\mathbb{E}[e_x^c(T)]$ and $\mathbb{E}[e_{x,T}^p]$, for females and males aged $x = 65$ at times $1966 \leq T \leq 2050$ under the ACF model. The solid lines are estimated with the fitted mortality rates. The solid lines marked by crosses represent Monte Carlo estimates. The solid lines marked by circles refer to the LSMC estimates.

Table 7 Expected cohort and period lifespan disparity, $\mathbb{E}[e_x^{c,\dagger}(T)]$ and $\mathbb{E}[e_{x,T}^{p,\dagger}]$, for females and males aged $x = 65$ at time T under the ACF model.

		female	male
$T = 2017$	period	7.64	7.85
	cohort	8.10	8.43
$T = 2028$	period	7.64	7.88
	cohort	8.02	8.41
$T = 2039$	period	7.62	7.89
	cohort	7.92	8.35
$T = 2050$	period	7.58	7.88
	cohort	7.82	8.27

Monte Carlo averaging, ignoring future improvements in mortality results in a lower level. The further period-based projection following 2017 is only slightly decreasing for females and essentially stable for males.

To conclude the analysis, Figure 13 compares on a single plot the joint evolution of cohort life expectancy and lifespan disparity for males and females under the ACF model.

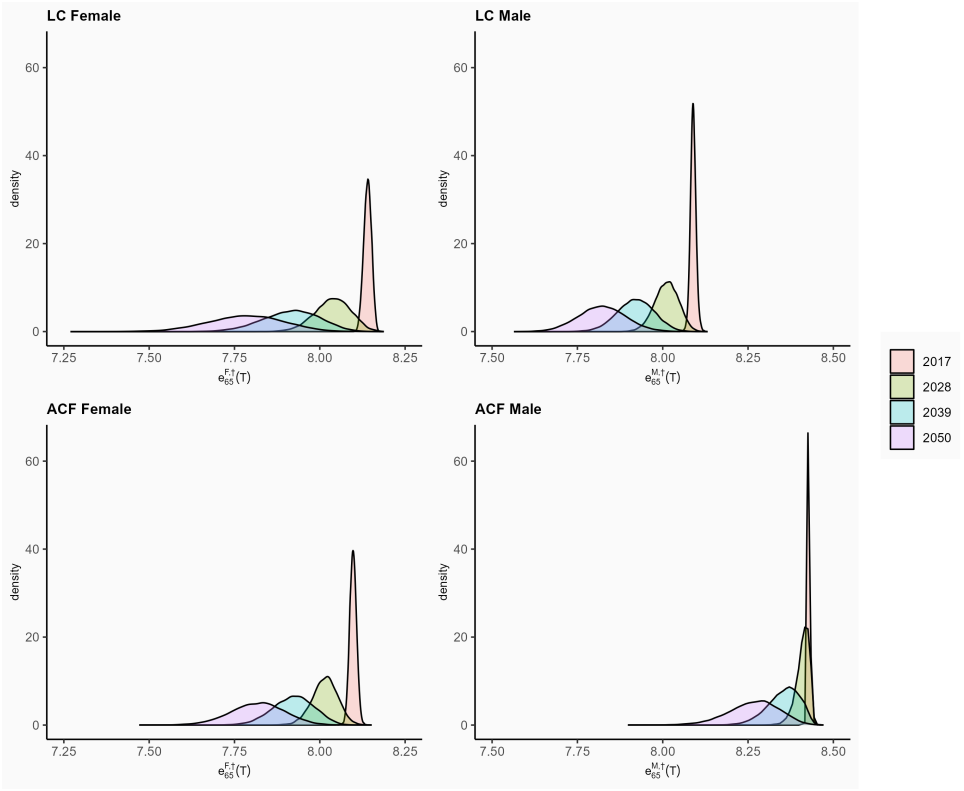

Fig. 8 Probability density function of cohort lifespan disparity $e_x^{\dagger,c}(T)$ for females (left) and males (right) aged $x = 65$ at times $T = 2017, 2028, 2039, 2050$. LC model (top), ACF model (bottom).

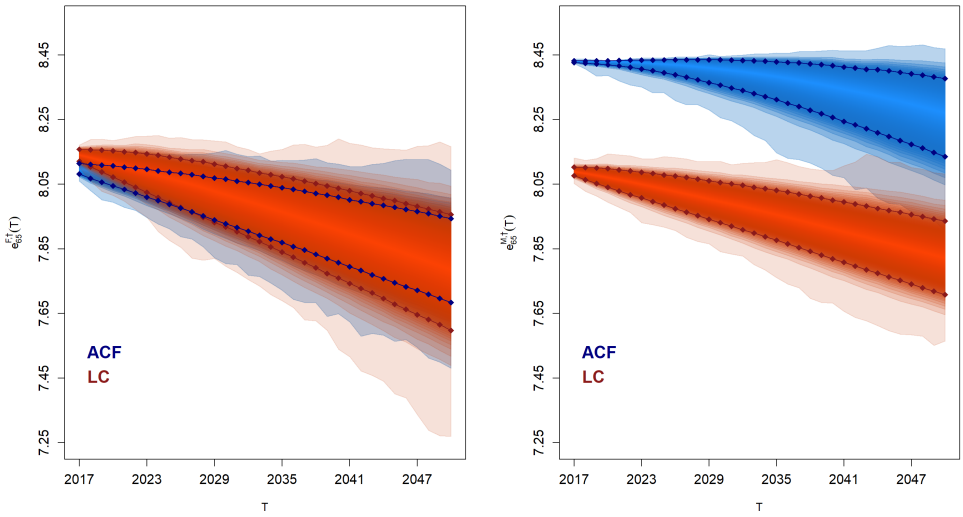

Fig. 9 Fan charts of the distribution of cohort lifespan disparity $e_x^{c,\dagger}(T)$ for females (left) and males (right) aged $x = 65$ at times $2017 \leq T \leq 2050$. LC model (red) and ACF model (blue).

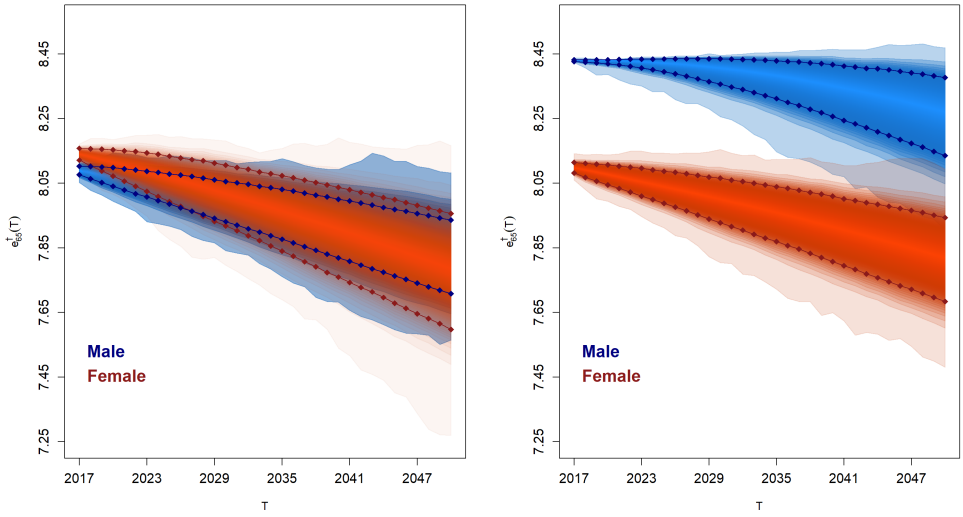

Fig. 10 Fan charts of the distribution of cohort lifespan disparity $e_x^{c,\dagger}(T)$ for females (red) and males (blue) aged $x = 65$ at times $2017 \leq T \leq 2050$. LC model (left) and ACF model (right).

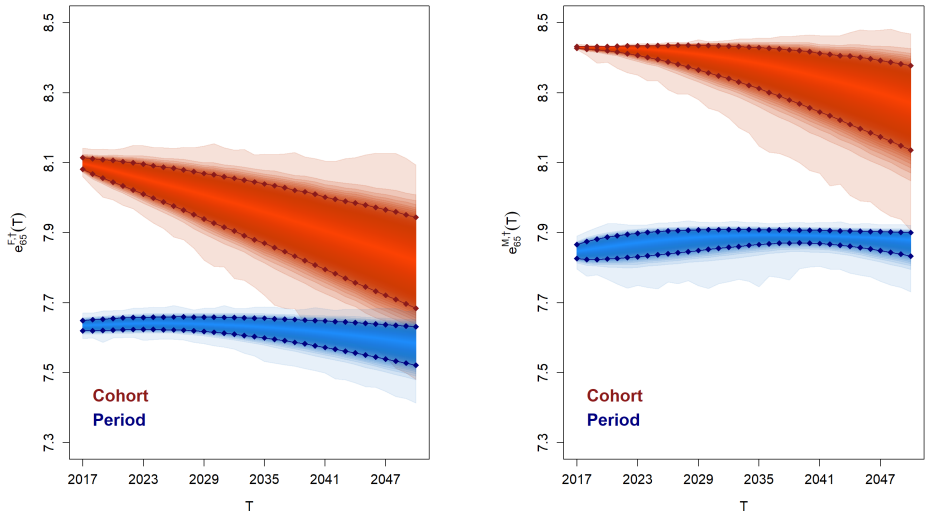

Fig. 11 Fan charts of the distribution of cohort (red) and period (blue) lifespan disparity, $e_x^{c,\dagger}(T)$ and $e_{x,T}^{p,\dagger}$, for females (left) and males (right) aged $x = 65$ at times $2017 \leq T \leq 2050$ under the ACF model.

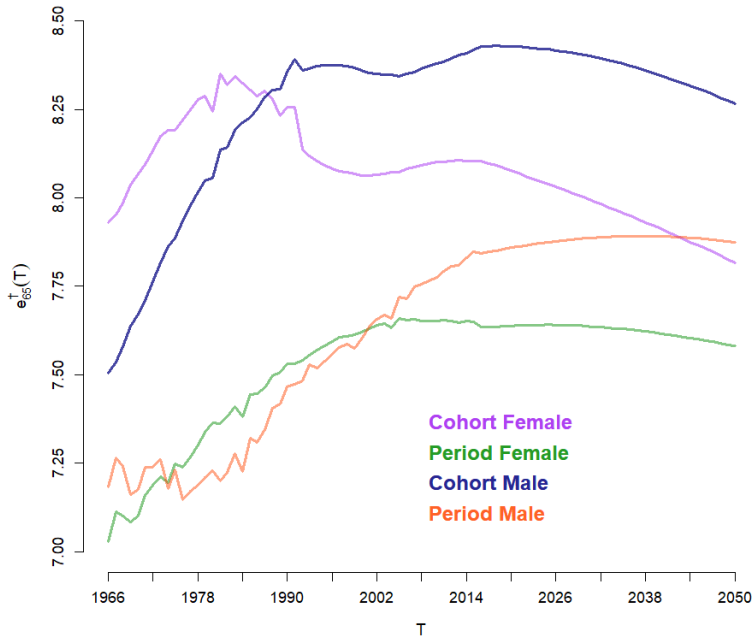

Fig. 12 Expected cohort and period lifespan disparities, $\mathbb{E}[e_x^{c,\dagger}(T)]$ and $\mathbb{E}[e_{x,T}^{p,\dagger}]$, for females and males aged $x = 65$ at times $1966 \leq T \leq 2050$ under the ACF model.

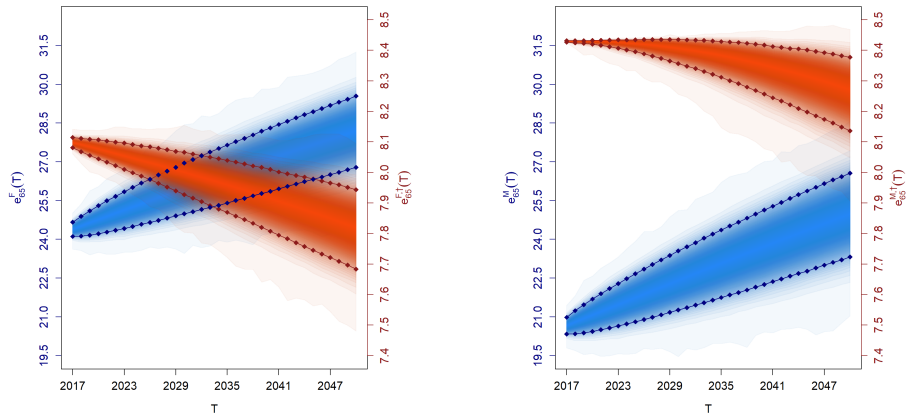

Fig. 13 Fan charts of the distribution of cohort life expectancy $e_x^c(T)$ (blue) and lifespan disparity $e_x^{c,\dagger}(T)$ (red) for females (left) and males (right) aged $x = 65$ at times $2017 \leq T \leq 2050$ under the ACF model.

5 Conclusions

In this paper we have addressed the ever-prominent issue of how to evaluate and forecast future longevity dynamics. In particular, we have focused on the analysis of the past and future evolution of two relevant longevity measures, which are usually taken into account by both demographic and actuarial studies, life expectancy and lifespan disparity. Our results have proved to be in line with those already presented in literature; indeed, we have recognised an ever-increasing trend in future life expectancy levels, and simultaneously a decreasing pattern in the future lifespan disparity for the male and female Italian population. However, in contrast to the usual period-based valuation approach, this study has been conducted by exploiting a cohort perspective. In this regard, even if period- and cohort-based valuations describe similar general trends of the two measures, we have seen how the first approach may not be able to detect promptly unexpected mortality developments, and so it may not effectively describe the actual life course.

Furthermore, we have compared the forecasting differences between single and multi-population mortality models; indeed, we have shown how the choice of the mortality model is crucial to effectively evaluate longevity risk.

Finally, we have proposed a very flexible tool to solve the involved conditional expectations, i.e., the Least-Squares Monte Carlo. The latter, indeed, has strongly decreased the computational effort which would have been required by a straightforward nested simulations method, thus allowing to evaluate more complex longevity measures such as the lifespan disparity.

To conclude, we want to strengthen the idea that the proposed methodology can be used for any other longevity index involving conditional arguments, where cohort measurements are often replaced by period ones for computational simplicity.

Acknowledgements

Anna Rita Bacinello, Pietro Millossovich and Fabio Viviano acknowledge co-funding from the Italian Ministry of University and Research, PRIN 2022 - Project number 2022FWZ2CR: "Building resilience to emerging risks in financial and insurance markets". This resource was co-financed by the Italian Ministry of University and Research [DD 967 30.06.2023]. Fabio Viviano gratefully acknowledges the financial support of the PNRR project "Italian Ageing, Age-It" (PE 00000015 - CUP H23C22000870006) and of the Italian Ministry of University and Research, which partially funded this work.
Earlier versions have been presented at the University of Alcalá, the University of Lausanne, the 11th Conference in Actuarial Science and Finance on Samos, the MLISTRAL Conference at CIRM-Marseille, the XXVI Congress on Insurance: Mathematics & Economics, the Longevity 18 Conference. We thank two anonymous referees and the editors for their comments, which greatly improved the paper.

Declarations

Competing interests

The authors declare none.

Appendix A Expected years of life lost and General Biometric Index

The information structure requires a filtration $(\mathcal{F}_t)_{t\geq 0}$ such that $\mathcal{F}_T$ includes the knowledge of the mortality rates $m_{x;t}$ with $t \leq T$ and all x. Further, each residual lifetime $\tau_x(T)$ is a stopping time in the filtration $(\mathcal{F}_{T+h})_{h\geq 0}$, for all integer age x. Let $\mathcal{M}$ represent the information resulting from the observation of all mortality rates, that is $m_{x;t}$ for all x and t.

The two alternative expressions for the lifespan disparity mentioned in Section 2, namely Eq. (9) and (10), are proved here.

$$\begin{aligned} e_x^{\dagger,\,c}(T) &= \mathbb{E}_T\left[e^c_{x+\tau_x(T)}\left(T+\tau_x(T)\right)\right] \\ &= \mathbb{E}_T\left[\sum_{k=0}^{\infty} \mathbb{1}_{\{\tau_x(T)=k\}} e^c_{x+k}(T+k)\right] \\ &= \mathbb{E}_T\left[\sum_{k=0}^{\infty} \mathbb{1}_{\{\tau_x(T)=k\}} \mathbb{E}_{T+k}\left[\sum_{h=1}^{\infty} e^{-\sum_{j=0}^{h-1} m_{x+k+j;T+k+j}}\right]\right]. \end{aligned}$$

Note that $\{\tau_x(T)=k\} \in \mathcal{F}_{T+k}$ for all $k \geq 0$. Then, through repeated applications of the linearity and Tower property, the lifespan disparity can be further expressed as

$$\begin{aligned} e_x^{\dagger,\,c}(T) &= \sum_{k=0}^{\infty} \mathbb{E}_T\left[\mathbb{1}_{\{\tau_{x,T}=k\}} \sum_{h=1}^{\infty} e^{-\sum_{j=0}^{h-1} m_{x+k+j;T+k+j}}\right] \\ &= \sum_{k=0}^{\infty} \mathbb{E}_T\left[\mathbb{E}_T\left[\mathbb{1}_{\{\tau_{x,T}=k\}} \sum_{h=1}^{\infty} e^{-\sum_{j=0}^{h-1} m_{x+k+j;T+k+j}} \mid \mathcal{M}\right]\right] \\ &= \sum_{k=0}^{\infty} \mathbb{E}_T\left[\mathbb{P}_T\left(\tau_{x,T}=k \mid \mathcal{M}\right) \sum_{h=1}^{\infty} e^{-\sum_{j=0}^{h-1} m_{x+k+j;T+k+j}}\right] \\ &= \sum_{k=0}^{\infty} \mathbb{E}_T\left[e^{-\sum_{j=0}^{k-1} m_{x+j;T+j}}\left(1-e^{-m_{x+k;T+k}}\right) \sum_{h=1}^{\infty} e^{-\sum_{j=0}^{h-1} m_{x+k+j;T+k+j}}\right] \\ &= \sum_{k=0}^{\infty} \mathbb{E}_T\left[\left(1-e^{-m_{x+k;T+k}}\right) \sum_{h=1}^{\infty} e^{-\sum_{j=0}^{k+h-1} m_{x+j;T+j}}\right] \\ &= \mathbb{E}_T\left[\sum_{k=0}^{\infty}\left(1-e^{-m_{x+k;T+k}}\right) \sum_{h=1}^{\infty} e^{-\sum_{j=0}^{k+h-1} m_{x+j;T+j}}\right], \end{aligned}$$

that is Eq. (9).

Now, starting from one of the latest expressions, and again using the Tower property,

$$
\begin{aligned}
e_x^{\dagger,\,c}(T) &= \mathbb{E}_T\left[\sum_{k=0}^{\infty}(1-e^{-m_{x+k;T+k}})\sum_{h=1}^{\infty}e^{-\sum_{j=0}^{k+h-1}m_{x+j;T+j}}\right] \\
&= \sum_{k=0}^{\infty}\mathbb{E}_T\left[\mathbb{E}_{T+k}\left[e^{-\sum_{j=0}^{k-1}m_{x+j;T+j}}(1-e^{-m_{x+k;T+k}})\sum_{h=1}^{\infty}e^{-\sum_{j=0}^{h-1}m_{x+k+j;T+k+j}}\right]\right] \\
&= \sum_{k=0}^{\infty}\mathbb{E}_T\left[e^{-\sum_{j=0}^{k-1}m_{x+j;T+j}}(1-e^{-m_{x+k;T+k}})\mathbb{E}_{T+k}\left[\sum_{h=1}^{\infty}e^{-\sum_{j=0}^{h-1}m_{x+k+j;T+k+j}}\right]\right] \\
&= \mathbb{E}_T\left[\sum_{k=0}^{\infty}e^{-\sum_{j=0}^{k-1}m_{x+j;T+j}}(1-e^{-m_{x+k;T+k}})e_{x+k}^{c}(T+k)\right],
\end{aligned}
$$

that is Eq. (10).

Appendix B The LSMC algorithm

The LSMC approach is essentially a simulation-based method combined with regression models. In what follows, we briefly describe the proposed algorithms to approximate the distribution of life expectancy and lifespan disparity for a generic cohort aged x at a future time T. A set of M basis functions $\boldsymbol{\phi} = (\phi_1, \ldots, \phi_M) : \mathbb{R}^r \to \mathbb{R}^M$ is needed, where r is the number of state variables in the vector X_t.

B.1 Future cohort life expectancy

Let us consider an individual aged x at the future time T, assuming that time $t = 0$ is today. To evaluate Eq. (5), the algorithm runs as follows:

1. Simulate n trajectories of the state variables:

   $$X_t^{(j)}, \quad t \geq 0,\, j = 1, \ldots, n;$$

   then obtain, through Eq. (12), simulation of the mortality rates

   $$m_{x+k;T+k}^{(j)}, \quad k = 1, \ldots, \omega - x - 1,$$

   where ω is the ultimate age.
2. Calculate

   $$E_x^{c,(j)}(T) = \frac{1}{2} + \sum_{h=1}^{\omega-x} e^{-\sum_{k=0}^{h-1} m_{x+k;T+k}^{(j)}}$$

   for $j = 1, \ldots, n$.

3. Regress
$$\left\{E_x^{c,(j)}(T)\right\}_j \quad \text{on} \quad \left\{\boldsymbol{\phi}(X_T^{(j)})\right\}_j,$$
to get regression coefficients $\hat{\beta}_1, \ldots, \hat{\beta}_M$.
4. Obtain n simulations of $e_x^c(T)$ by
$$\hat{e}_x^{c,(j)}(T) = \sum_{l=1}^{M} \hat{\beta}_l \phi_l(X_T^{(j)}), \qquad j = 1, \ldots, n.$$

B.2 Iterative LSMC for the future cohort lifespan disparity

Concerning the approximation of the future lifespan disparity distribution, we apply an LSMC algorithm to Eq. (10). To this end, multiple conditional future life expectancies need to be evaluated. The algorithm runs as follows:

1. Simulate n trajectories of the state variables:
$$X_t^{(j)}, \quad t \geq 0,\, j = 1, \ldots, n;$$
then obtain, through Eq. (12), simulation of the mortality rates
$$m_{x+k;T+k}^{(j)}, \quad k = 1, \ldots, \omega - x - 1.$$
2. Evaluate
$$\hat{e}_{x+h}^{c,(j)}(T+h), \quad h = 0, \ldots, \omega - x - 1,$$
using the algorithm described in B.1.
3. Compute
$$E_{x,T}^{\dagger,c,(j)} = \sum_{h=0}^{\omega-x-1} \hat{e}_{x+h}^{c,(j)}(T+h) \cdot e^{-\sum_{k=0}^{h-1} m_{x+k;T+k}^{(j)}} \cdot \left(1 - e^{-m_{x+h;T+h}^{(j)}}\right), \quad j = 1, \ldots, n.$$
4. Regress
$$\left\{E_{x,T}^{\dagger,c(j)}\right\}_j \quad \text{on} \quad \left\{\boldsymbol{\phi}(X_T^{(j)})\right\}_j,$$
to get regression coefficients $\hat{\beta}_1, \ldots, \hat{\beta}_M$.
5. Obtain n simulations of $e_x^{\dagger,c}(T)$ by
$$\hat{e}_x^{\dagger,c,(j)}(T) = \sum_{l=1}^{M} \hat{\beta}_l \phi_l(X_T^{(j)}), \qquad j = 1, \ldots, n.$$

References

[1] Bacinello AR, Millossovich P, Viviano F (2021) An efficient Monte Carlo based approach for the simulation of future annuity values. Research Paper DEAMS, n.2/2021. Available at http://hdl.handle.net/10077/32218

[2] Bacinello AR, Millossovich P, Viviano F (2022) A regression based approach for valuing longevity measures. In: Corazza M, Perna C, Pizzi C, et al (eds) Mathematical and Statistical Methods for Actuarial Sciences and Finance. Springer International Publishing, p. 44–49, Cham, pp 44–49, https://doi.org/https://doi.org/10.1007/978-3-030-99638-3_8

[3] Biffis E, Blake D, Pitotti L, et al (2016) The cost of counterparty risk and collateralization in longevity swaps. The Journal of Risk and Insurance 83(2):387–419. https://doi.org/https://doi.org/10.1111/jori.12055

[4] Boyer MM, Stentoft L (2013) If we can simulate it, we can insure it: An application to longevity risk management. Insurance: Mathematics and Economics 52(1):35–45. https://doi.org/https://doi.org/10.1016/j.insmatheco.2012.10.003

[5] Cairns AJ (2011) Modelling and management of longevity risk: Approximations to survivor functions and dynamic hedging. Insurance: Mathematics and Economics 49(3):438–453. https://doi.org/https://doi.org/10.1016/j.insmatheco.2011.06.004

[6] Cairns AJ, Blake D, Dowd K, et al (2011) Bayesian stochastic mortality modelling for two populations. ASTIN Bulletin 41(1):29–59. https://doi.org/10.2143/AST.41.1.2084385

[7] Cairns AJG, Blake D, Dowd K (2006) A two-factor model for stochastic mortality with parameter uncertainty: Theory and calibration. Journal of Risk and Insurance 73(4):687–718. https://doi.org/https://doi.org/10.1111/j.1539-6975.2006.00195.x

[8] Cairns AJG, Blake D, Dowd K, et al (2009) A quantitative comparison of stochastic mortality models using data from England and Wales and the United States. North American Actuarial Journal 13(1):1–35. https://doi.org/10.1080/10920277.2009.10597538

[9] Carrière JF (1996) Valuation of the early-exercise price for options using simulations and nonparametric regression. Insurance: Mathematics and Economics 19(1):19–30. https://doi.org/https://doi.org/10.1016/S0167-6687(96)00004-2

[10] Chen RY, Millossovich P (2018) Sex-specific mortality forecasting for UK countries: a coherent approach. European Actuarial Journal 8:69–95. https://doi.org/https://doi.org/10.1007/s13385-017-0164-0

[11] Debon A, Montes F, Martínez-Ruiz F (2011) Statistical methods to compare mortality for a group with non-divergent populations: an application to Spanish regions. European Actuarial Journal 1:291–308. https://doi.org/10.1007/s13385-011-0043-z

[12] Dowd K, Blake D, Cairns AJ (2010) Facing up to uncertain life expectancy: The longevity fan charts. Demography 47(1):67–78. https://doi.org/https://doi.org/10.1353/dem.0.0083

[13] Dowd K, Blake D, Cairns AJG (2011) A computationally efficient algorithm for estimating the distribution of future annuity values under interest-rate and longevity risks. North American Actuarial Journal 15(2):237–247. https://doi.org/10.1080/10920277.2011.10597619

[14] Dowd K, Cairns AJG, Blake D, et al (2011) A gravity model of mortality rates for two related populations. North American Actuarial Journal 15(2):334–356. https://doi.org/10.1080/10920277.2011.10597624

[15] Edwards RD, Tuljapurkar S (2005) Inequality in life spans and a new perspective on mortality convergence across industrialized countries. Population and Development Review 31(4):645–674. https://doi.org/https://doi.org/10.1111/j.1728-4457.2005.00092.x

[16] Ghalehjooghi AS, Lyu P (2022) Socio-economic differentiation in experienced mortality modelling and its pricing implications. European Actuarial Journal 12(1):161–188. https://doi.org/10.1007/s13385-021-00282-1

[17] Ghalehjooghi AS, Pelsser A (2021) Time-consistent and market-consistent actuarial valuation of the participating pension contract. Scandinavian Actuarial Journal 2021(4):266–294. https://doi.org/10.1080/03461238.2020.1832911

[18] Glasserman P (2004) Monte Carlo methods in financial engineering. Springer, New York, https://doi.org/https://doi.org/10.1007/978-0-387-21617-1

[19] Goldman N, Lord G (1986) A new look at entropy and the life table. Demography 23(2):275–282. https://doi.org/https://doi.org/10.2307/2061621

[20] Guillot M (2011) Period versus cohort life expectancy. In: Rogers RG, Crimmins EM (eds) International Handbook of Adult Mortality. Springer Netherlands, Dordrecht, p 533–549, https://doi.org/10.1007/978-90-481-9996-9_25

[21] Ha H, Bauer D (2022) A least-squares Monte Carlo approach to the estimation of enterprise risk. Finance and Stochastics 26:417–459. https://doi.org/https://doi.org/10.1007/s00780-022-00478-7

[22] Haberman S, Renshaw A (2011) A comparative study of parametric mortality projection models. Insurance: Mathematics and Economics 48(1):35–55. https://doi.org/https://doi.org/10.1016/j.insmatheco.2010.09.003

[23] Hunt A, Blake D (2021) On the structure and classification of mortality models. North American Actuarial Journal 25(S1):215–234. https://doi.org/https://doi.org/10.1080/10920277.2019.1649156

[24] Hyndman RJ, Booth H, Yasmeen F (2013) Coherent mortality forecasting: The product-ratio method with functional time series models. Demography 50(1):261–283. https://doi.org/10.1007/s13524-012-0145-5

[25] Janssen F (2018) Advances in mortality forecasting: introduction. Genus 74:21. https://doi.org/https://doi.org/10.1186/s41118-018-0045-7

[26] Jevtić P, Regis L (2019) A continuous-time stochastic model for the mortality surface of multiple populations. Insurance: Mathematics and Economics 88:181–195. https://doi.org/https://doi.org/10.1016/j.insmatheco.2019.07.001

[27] Keyfitz N, Caswell H (2005) Applied Mathematical Demography, 3rd edn. Springer-Verlag, New York, NY, https://doi.org/https://doi.org/10.1007/b139042

[28] Kleinow T (2015) A common age effect model for the mortality of multiple populations. Insurance: Mathematics and Economics 63:147–152. https://doi.org/https://doi.org/10.1016/j.insmatheco.2015.03.023

[29] Lee RD, Carter LR (1992) Modeling and forecasting US mortality. Journal of the American Statistical Association 87(419):659–671. https://doi.org/https://doi.org/10.1080/01621459.1992.10475265

[30] Li J, Tickle L, Parr N (2016) A multi-population evaluation of the Poisson common factor model for projecting mortality jointly for both sexes. Journal of Population Research 33:333–360. https://doi.org/https://doi.org/10.1007/s12546-016-9173-0

[31] Li N, Lee R (2005) Coherent mortality forecasts for a group of populations: An extension of the Lee-Carter method. Demography 42(3):575–594. https://doi.org/https://doi.org/10.1353/dem.2005.0021

[32] Longstaff FA, Schwartz ES (2001) Valuing American options by simulation: A simple least-squares approach. The Review of Financial Studies 14(1):113–147. https://doi.org/10.1093/rfs/14.1.113

[33] Luciano E, Vigna E (2008) Mortality risk via affine stochastic intensities: calibration and empirical relevance. Belgian Actuarial Bulletin 8(1):5–16

[34] Nigri A, Levantesi S, Marino M (2021) Life expectancy and lifespan disparity forecasting: a long short-term memory approach. Scandinavian Actuarial Journal 2021(2):110–133. https://doi.org/10.1080/03461238.2020.1814855

[35] Niu G, Melenberg B (2014) Trends in mortality decrease and economic growth. Demography 51(5):1755–1773. https://doi.org/https://doi.org/10.1007/s13524-014-0328-3

[36] Rabbi A, Mazzuco S (2021) Mortality forecasting with the Lee–Carter method: Adjusting for smoothing and lifespan disparity. European Journal of Population 37:97–120. https://doi.org/10.1007/s10680-020-09559-9

[37] Renshaw A, Haberman S (2003) Lee–Carter mortality forecasting with age-specific enhancement. Insurance: Mathematics and Economics 33(2):255–272. https://doi.org/https://doi.org/10.1016/S0167-6687(03)00138-0

[38] Renshaw A, Haberman S (2006) A cohort-based extension to the Lee–Carter model for mortality reduction factors. Insurance: Mathematics and Economics 38(3):556–570. https://doi.org/https://doi.org/10.1016/j.insmatheco.2005.12.001

[39] Tilley JA (1993) Valuing American options in a path simulation model. Transactions of Society of Actuaries 45:499–520

[40] van Raalte AA, Caswell H (2013) Perturbation analysis of indices of lifespan variability. Demography 50:1615–1640. https://doi.org/https://doi.org/10.1007/s13524-013-0223-3

[41] Vaupel JW (1986) How change in age-specific mortality affects life expectancy. Population Studies 40:147–157. https://doi.org/https://doi.org/10.1080/0032472031000141896

[42] Vaupel JW, Zhang Z, van Raalte AA (2011) Life expectancy and disparity: an international comparison of life table data. BMJ Open 1(1). https://doi.org/10.1136/bmjopen-2011-000128

[43] Villegas AM, Haberman S, Kaishev VK, et al (2017) A comparative study of two-population models for the assessment of basis risk in longevity hedges. ASTIN Bulletin 47(3):631–679. https://doi.org/10.1017/asb.2017.18

[44] Villegas AM, Kaishev VK, Millossovich P (2018) **StMoMo**: An **R** package for stochastic mortality modeling. Journal of Statistical Software 84(3):1–38. https://doi.org/https://doi.org/10.18637/jss.v084.i03

[45] Wilmoth J (2000) Demography of longevity: past, present, and future trends. Experimental gerontology 35(9-10):1111—1129. https://doi.org/10.1016/s0531-5565(00)00194-7

[46] Wilmoth J, Horiuchi S (1999) Rectangularization revisited: Variability of age at death within human populations. Demography 36:475–495. https://doi.org/https://doi.org/10.2307/2648085

[47] Yang B, Li J, Balasooriya U (2016) Cohort extensions of the Poisson common factor model for modelling both genders jointly. Scandinavian Actuarial Journal 2016(2):93–112. https://doi.org/10.1080/03461238.2014.908411